Inorganic Chemistry

Article

Silver Delafossite Oxides

William C. Sheets,[†] Evan S. Stampler,[†] Mariana I. Bertoni,[‡] Makoto Sasaki,[§] Tobin J. Marks,[†,‡]
Thomas O. Mason,[‡] and Kenneth R. Poeppelmeier*,[†]

*Departments of Chemistry and of Materials Science and Engineering, Northwestern University,
Evanston, Illinois 60208, and, Department of Materials Science and Engineering, Muroran
Institute of Technology, 27-1 Mizumoto, Muroran, Hokkaido 050-8585, Japan*

A single-step, low-temperature (<210 °C) and -pressure (<20 atm) hydrothermal method has been developed to synthesize a series of silver delafossites, $AgBO_2$ (B = Al, Ga, Sc, and In). Experimental and computational studies were performed to understand the optical and electric properties of these silver delafossites, including the first in-depth study of $AgAlO_2$ and $AgScO_2$. Their properties were examined as a function of the trivalent cation radius and compared to those of copper delafossites to elucidate the role of both the A- and B-site cations. While optical band gaps for silver delafossites were larger and visible light absorption was lower than values previously reported for polycrystalline powder samples of copper delafossites, the conductivities of silver delafossites are similar or lower. Electronic structure calculations indicate that these properties are due to the scarcity of silver 4d states just below the valence band maximum.

Introduction

The physical properties of numerous delafossites were first reported as part of a large study on the synthesis, structure, and electrical transport properties of delafossites by Rogers, Shannon, and Prewitt.[1–3] Later, Benko and Koffyberg reported the electrical and optical properties of certain copper delafossites in a series of papers.[4–7] In 1997, interest in delafossites was rekindled when a seminal paper by Kawazoe and co-workers revealed that a 500 nm thick film of $CuAlO_2$ transmitted 70% of visible light and exhibited p-type conductivity of 0.95 S cm^{-1}.[8] Since then, delafossites, especially the copper and silver members, have received considerable attention owing to their application as transparent conducting oxides.[9,10] Particular emphasis has been placed on optimizing their optical and electrical properties through proper selection of the parent delafossite, aliovalent dopant, and/or control of the oxygen stoichiometry. Because of their compositional versatility, delafossites also have been studied intensely as catalysts,[11–14] luminescent materials,[15,16] batteries,[17] and thermoelectrics.[18–21] Recent photocatalytic applications have exploited the sensitivity of delafossites to

* To whom correspondence should be addressed. E-mail: krp@northwestern.edu.
  † Department of Chemistry.
 ‡ Department of Materials Science and Engineering.
  § Muroran Institute of Technology.

(1) Shannon, R. D.; Rogers, D. B.; Prewitt, C. T. *Inorg. Chem.* **1971**, *10*(4), 713–718.
(2) Prewitt, C. T.; Shannon, R. D.; Rogers, D. B. *Inorg. Chem.* **1971**, *10*(4), 719–723.
(3) Rogers, D. B.; Shannon, R. D.; Prewitt, C. T.; Gillson, J. L. *Inorg. Chem.* **1971**, *10*(4), 723–727.
(4) Benko, F. A.; Koffyberg, F. P. *J. Phys. Chem. Solids* **1984**, *45*(1), 57–59.
(5) Benko, F. A.; Koffyberg, F. P. *Can. J. Phys.* **1985**, *63*(10), 1306–1308.
(6) Benko, F. A.; Koffyberg, F. P. *Phys. Status Solidi A* **1986**, *94*(1), 231–234.
(7) Benko, F. A.; Koffyberg, F. P. *J. Phys. Chem. Solids* **1987**, *48*(5), 431–434.

(8) Kawazoe, H.; Yasukawa, M.; Hyodo, H.; Kurita, M.; Yanagi, H.; Hosono, H. *Nature (London)* **1997**, *389*(6654), 939–942.
(9) Ginley, D. S.; Bright, C. *MRS Bull.* **2000**, *25*(8), 15–21.
(10) Kawazoe, H.; Yanagi, H.; Ueda, K.; Hosono, H. *MRS Bull.* **2000**, *25*(8), 28–36.
(11) Carcia, P. F.; Shannon, R. D.; Bierstedt, P. E.; Flippen, R. B. *J. Electrochem. Soc.* **1980**, *127*(9), 1974–1978.
(12) Monnier, J. R.; Hanrahan, M. J.; Apai, G. *J. Catal.* **1985**, *92*(1), 119–126.
(13) Christopher, J.; Swamy, C. S. *J. Mater. Sci.* **1992**, *27*(5), 1353–1356.
(14) Domen, K.; Ikeda, S.; Takata, T.; Tanaka, A.; Hara, M.; Kondo, J. N. *Appl. Energy* **2000**, *67*(1–2), 159–179.
(15) Doumerc, J. P.; Parent, C.; Chao, Z. J.; Le Flem, G.; Ammar, A. *J. Less-Common Met.* **1989**, *148*, 333–337.
(16) Jacob, A.; Parent, C.; Boutinaud, P.; LeFlem, G.; Doumerc, J. P.; Ammar, A.; Elazhari, M.; Elaatmani, M. *Solid State Commun.* **1997**, *103*(9), 529–532.
(17) Nagaura, T. *Prog. Batteries Solar Cells* **1982**, *4*, 105–107.
(18) Isawa, K.; Yaegashi, Y.; Ogota, S.; Nagano, M.; Sudo, S.; Yamada, K.; Yamauchi, H. *Phys. Rev. B: Condens. Matter* **1998**, *57*(13), 7950–7954.

light in the visible region, and the variability in their optical band gaps for different A- and B-site cation combinations offers many further applications.[22–27] For copper delafossites, the effect of altering the B-site cation on both the optical and electrical properties has been investigated extensively.[7,28–30] In comparison, the optical and electrical properties of silver delafossites are not well understood, and some disagreement exists on the reported optical properties. For example, Vanaja et al. reported an optically measured band gap of 4.12 eV for a thin film sample of $AgGaO_2$,[31] whereas Maruyama and co-workers reported an optically measured band gap of 2.4 eV for a polycrystalline powder sample.[24] Similar optically measured band-gap anomalies have been observed in copper delafossites and have been studied by absorption spectroscopy and electronic structure calculations.[32–34]

The layered delafossite $A^+B^{3+}O_2$ structure, as exemplified by the parent delafossite mineral, $CuFeO_2$,[35,36] maintains the expected valences for the monovalent A-site cations (Ag^+ and Cu^+) and trivalent B-site cations [$0.535 < r(B^{3+}) < 1.03$ Å].[37,38] This structure consists of alternate layers of two-dimensional close-packed A cations with linear $O–A^+–O$ bonds and slightly distorted edge-shared $B^{3+}O_6$ octahedra (Figure 1).[2] Furthermore, each oxygen is coordinated by four cations (one A^+ and three B^{3+}) in a pseudotetrahedral arrangement. Depending on the stacking of the double layers (close-packed A cations and BO_6 octahedra), two polytypes are possible. The 3R polytype consists of "AaBbCcAaBbCc" stacking along the *c* axis and has rhombohedral symmetry
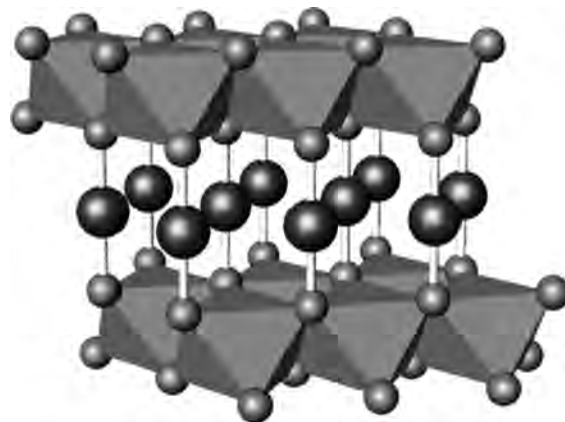
Figure 1. Schematic representation of the delafossite structure (ABO_2). The gray polyhedra and black spheres represent edge-shared $B^{3+}O_6$ distorted octahedra and linearly coordinated A^+ cations, respectively.

with the space group $R\bar{3}m$, whereas the 2H polytype consists of an alternate "AaBbAaBb" stacking sequence in the $P6_3/mmc$ space group.

The synthesis of silver delafossites by high-temperature ceramic methods never occurs in open systems because Ag_2O decomposes, owing to its low free energy of formation, before any appreciable reaction can occur. This low value ($\Delta F_f = -2.6$ kcal/mol) results in decomposition to silver metal and oxygen at a temperature of 300 °C.[1] Therefore, alternative synthetic methods, including high-oxygen-pressure solid-state, metathetical (cation-exchange), oxidizing flux, and hydrothermal reactions, have been used to generate silver delafossites. For example, silver ferrate ($AgFeO_2$), the first reported silver delafossite, was prepared at low temperatures (~100 °C) by Krause and Gawryck from the combination of a "meta-ferric hydroxide gel" (γ-FeOOH) and Ag_2O in a boiling NaOH solution.[39] To prepare small single crystals, Croft et al. employed thin-walled platinum tubes at higher temperatures (400 °C) and pressures (2700 atm) to synthesize $AgFeO_2$ from Ag_2O and Fe_2O_3 and therefore took advantage of a closed system (hydrothermal conditions) to prevent decomposition of Ag_2O.[40] Later, Shannon et al. reported the first comprehensive study of three closed-system syntheses (metathetical, oxidizing flux, and hydrothermal) to generate numerous single-crystal and powder samples of delafossites, including silver delafossites.[1] In general, the techniques involved low temperatures (e.g., metathesis reactions with the formation of a fused salt byproduct), oxidizing conditions (e.g., solid-state reactions at high pressures of internally generated oxygen), or both (e.g., hydrothermal or oxidizing flux reactions). There was no single technique reported, however, that could be used to obtain the various silver delafossites and the authors noted limitations for each synthetic method. First, the metathesis reactions always led to the formation of highly stable silver halides with little to no delafossite present. Oxidizing flux reactions, where the flux was removed with a postsynthetic leaching step, resulted in higher yields of the delafossite

(19) Yagi, H.; Seo, W.-S.; Koumoto, K. *Key Eng. Mater.* **2000**, *181–182*, 63–66.
(20) Koumoto, K.; Koduka, H.; Seo, W.-S. *J. Mater. Chem.* **2001**, *11*(2), 251–252.
(21) Takahashi, Y.; Matsushita, H.; Katsui, A. *Mater. Sci. Forum* **2007**, *534–536*(2), 1081–1084(Progress in Powder Metallurgy).
(22) Bessekhouad, Y.; Trari, M.; Doumerc, J. P. *Int. J. Hydrogen Energy* **2003**, *28*(1), 43–48.
(23) Koriche, N.; Bouguelia, A.; Aider, A.; Trari, M. *Int. J. Hydrogen Energy* **2005**, *30*, 693.
(24) Maruyama, Y.; Irie, H.; Hashimoto, K. *J. Phys. Chem. B* **2006**, *110*(46), 23274–23278.
(25) Trari, M.; Bouguelia, A.; Bessekhouad, Y. *Sol. Energy Mater. Sol. Cells* **2006**, *90*(2), 190–202.
(26) Saadi, S.; Bouguelia, A.; Derbal, A.; Trari, M. *J. Photochem. Photobiol., A* **2007**, *187*(1), 97–104.
(27) Brahimi, R.; Bessekhouad, Y.; Bouguelia, A.; Trari, M. *J. Photochem. Photobiol., A* **2007**, *186*(2–3), 242–247.
(28) Nagarajan, R.; Duan, N.; Jayaraj, M. K.; Li, J.; Vanaja, K. A.; Yokochi, A.; Draeseke, A.; Tate, J.; Sleight, A. W. *Int. J. Inorg. Mater.* **2001**, *3*(3), 265–270.
(29) Ingram, B. J.; Harder, B. J.; Hrabe, N. W.; Mason, T. O.; Poeppelmeier, K. R. *Chem. Mater.* **2004**, *16*(26), 5623–5629.
(30) Marquardt, M. A.; Ashmore, N. A.; Cann, D. P. *Thin Solid Films* **2006**, *496*(1), 146–156.
(31) Vanaja, K. A.; Ajimsha, R. S.; Asha, A. S.; Jayaraj, M. K. *Appl. Phys. Lett.* **2006**, *88*(21), 212103/1–212103/3.
(32) Pellicer-Porres, J.; Segura, A.; Gilliland, A. S.; Munoz, A.; Rodriguez-Hernandez, P.; Kim, D.; Lee, M. S.; Kim, T. Y. *Appl. Phys. Lett.* **2006**, *88*(18), 181904/1–181904/3.
(33) Makhova, L.; Wett, D.; Lorenz, M.; Konovalov, I. *Phys. Status Solidi A* **2006**, *203*(11), 2861–2866.
(34) Nie, X.; Wei, S.-H.; Zhang, S. B. *Phys. Rev. Lett.* **2002**, *88*(6), 066405/1–066405/4.
(35) Soller, W.; Thompson, A. J. *Phys. Rev.* **1935**, *47*, 644.
(36) Pabst, A. *Am. Mineral.* **1946**, *31*, 539–546.
(37) Shannon, R. D.; Prewitt, C. T. *Acta Crystallogr., Sect. B* **1969**, *25*(Pt. 5), 925–946.
(38) Shannon, R. D. *Acta Crystallogr., Sect. A* **1976**, *A32*(5), 751–767.

(39) Krause, A.; Gawryck, S. *Z. Anorg. Allg. Chem.* **1938**, *238*, 406–412.
(40) Croft, W. J.; Tombs, N. C.; England, R. E. *Acta Crystallogr., Sect. A* **1964**, *17*, 313–314.

phase, but the presence of a second phase was also reported for certain compositions. Hydrothermal reactions, carried out at 500−700 °C with 3000 atm of externally applied pressure, produced small amounts of the target delafossite in a mixture with Ag_2O, which was easily removed by leaching the mixture in dilute nitric acid. As with most high-pressure and -temperature hydrothermal techniques, the use of sealed, thin-walled gold or platinum tubes limited the mass yield of the reaction.

Small amounts of $AgAlO_2$ and $AgScO_2$ have been synthesized previously by high-temperature and -pressure reactions.[1,41] However, the optical and electrical properties of these silver delafossites have not been studied in-depth. Here, we demonstrate that low-temperature hydrothermal techniques originally developed for the synthesis of copper delafossites can be exploited to access numerous silver delafossites. In this approach, the hydrothermal synthesis of the desired product was enabled by controlling the pH using a NaOH mineralizer. As a result, we report here an experimental and computational analysis of the optical and electrical properties of silver delafossites. The optical and electrical properties of these delafossites are presented and compared with each other and copper delafossites, where A = Ag and Cu and B = Al, Ga, Sc, and In, which has permitted a discussion on the influence that both the A- and B-site cations has on their properties.

Experimental Section

Synthesis. Polycrystalline silver delafossites were prepared from a direct hydrothermal reaction between silver oxide (99.99%, Alfa Aesar) and the appropriate B-site cation sesquioxide or trihydroxide (Supporting Information).[42–44] Stoichiometric amounts (0.8 g of total mass) of these reactants were placed along with fused NaOH into individual fluoro(ethylene−propylene) Teflon pouches. The effect of pH and temperature on product formation is discussed elsewhere.[44] For any individual preparation, multiple pouches were placed in each 125-mL poly(tetrafluoroethylene) (PTFE) Teflon-lined pressure vessel (Parr Instruments), which was then backfilled with 50 mL of distilled water. The pressure vessel was then sealed and heated to 150 °C, followed by a controlled incremental increase over 5 h to the desired reaction temperature, from 180 to 210 °C depending on the delafossite. This incremental temperature increase is necessary to prevent a rapid influx of water from rupturing the pouch.[44] The maximum temperature was held constant for 60 h with subsequent cooling to room temperature at 6 °C/h. After the latter step, the pouch was opened and polycrystalline products were recovered by filtration, followed by a deionized water rinse to remove any NaOH. To minimize any photochromic decomposition of the silver delafossites after drying, samples were wrapped in

aluminum foil and kept away from light. Reference copper delafossites ($CuAlO_2$, $CuGaO_2$, $CuScO_2$, and $CuInO_2$) were synthesized by literature methods.[45–47]

Powder X-ray Analysis. Powder X-ray diffraction (PXD) data were recorded on a Rigaku XDS 2000 diffractometer with Ni-filtered Cu Kα radiation operating at 40 kV and 20 mA. Data were collected in the 2θ range of 10−80° by scanning every 0.05° for 1 s. Where available, the PXD patterns were matched to their respective JCPDS files using the *Jade* software suite.[48] Samples not having a JCPDS file were matched to calculated PXD patterns generated from published crystallographic data by the *PowderCell* software suite.[49]

Composition Analysis. Cation ratios were determined by inductively coupled plasma atomic emission spectroscopy (ICP-AES). The polycrystalline powder samples were dissolved in HNO_3 at 80 °C for 3 h and then diluted to measurable concentrations (ppm) with deionized water. A Thermo Jarrell Ash Atomscan model 25 Sequential ICP spectrometer equipped with vacuum optics covering the spectral range from 160 to 850 nm was used in the current work. Three readings were taken per sample and averaged. Thermogravimetric analysis (TGA) was performed to determine the oxygen content of selected samples. Approximately 10–30 mg of material was reduced under flowing N_2 gas in a thermogravimetric analyzer model Q50 (TA Instruments), and the weight loss was determined precisely. The resultant products were analyzed by X-ray diffraction (XRD) to verify that the following general reaction occurred:

$$4Ag_{1+x}M^{3+}_{1+y}O_{2+\delta} \xrightarrow{\Delta} 4(1+x)Ag_{metal} + 2(1+y)M^{3+}_2O_3 +$$

$$(1 + 2\delta - 6y)O_2 \quad (1)$$
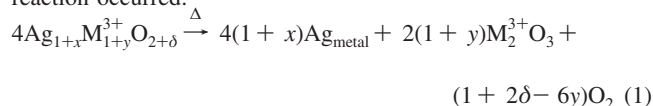
Electron Microscope Analysis. Electron microscopy studies of delafossites were carried out using a Hitachi S-4500 scanning electron microscope (SEM). To prepare SEM samples, polycrystalline samples were attached to an aluminum mount using carbon tape and coated with 5 nm of gold.

Optical Analysis. Optical data were obtained via diffuse reflectance. In a diffuse-reflectance experiment, the nonspecular component of reflection (i.e., radiation that has undergone multiple scattering events on different particles and returned to the sample surface) is measured relative to a standard.[50] The transition edge onset was used to estimate an optical gap. Diffuse-reflectance data were collected over the spectral range 200–800 nm using a Cary 500 scanning double-beam spectrophotometer equipped with an integrating sphere (110 mm in diameter; Cary 1E with Cary 1/3 attachment, Varian, Walnut Creek, CA). Baseline spectra were collected using pressed PTFE placed in the sample and reference beams. Data were collected with a scan rate of 300 nm/min, a data interval of 1 nm, an average time of 0.2 s, and a signal bandwidth of 3 nm. Pellets were mounted on a blackened sample mask. The reflectance data were translated into absorption data (α/S) by using an equation developed by Kubelka and Munk, $\alpha/S = (1−R)^2/2R$, where α is the absorption coefficient, S is the scattering coefficient, and R is the diffuse reflectance at a certain energy.[51]

Conductivity Measurements. The electrical conductivity of the as-prepared polycrystalline silver delafossites was obtained by the

(41) Brachtel, G.; Jansen, M. *Cryst. Struct. Commun.* **1981**, *10*(1), 173–174.
(42) Shahriari, D. Y.; Barnabe, A.; Mason, T. O.; Poeppelmeier, K. R. *Inorg. Chem.* **2001**, *40*(23), 5734–5735.
(43) Shahriari, D. Y.; Erdman, N.; Haug, U. T. M.; Zarzyczny, M. C.; Marks, L. D.; Poeppelmeier, K. R. *J. Phys. Chem. Solids* **2003**, *64*(9–10), 1437–1441.
(44) Sheets, W. C.; Mugnier, E.; Barnabe, A.; Marks, T. J.; Poeppelmeier, K. R. *Chem. Mater.* **2006**, *18*(1), 7–20.
(45) Ingram, B. J.; Mason, T. O.; Asahi, R.; Park, K. T.; Freeman, A. J. *Phys. Rev. B: Condens. Matter* **2001**, *64*(15), 155114/1–155114/7.
(46) Park, S.; Keszler, D. A. *J. Solid State Chem.* **2003**, *173*(2), 355–358.
(47) Koehler, B. U.; Jansen, M. *Z. Anorg. Allg. Chem.* **1986**, *543*, 73–80.
(48) *Jade*, 5.0; Materials Data Inc.: Livermore, CA, 1999.
(49) *PowderCell*, 2.4; Federal Institute for Materials Research and Testing: Berlin, Germany, 2000.
(50) Hecht, H. G. *Proceedings of the Symposium on Modern Aspects of Reflectance Spectroscopy*; Plenum Press New York, 1968; pp 1–26.
(51) Kubelka, P.; Munk, F. *Z. Tech. Phys. (Leipzig)* **1931**, *12*, 593.

powder-solution-composite (PSC) technique.[52] In this technique, the bulk conductivity of a ceramic powder is obtained by measuring the impedance spectra of composite slurries of the powder with electrolytic solutions of NaCl. Powder conductivity is obtained from a series of experiments in which the conductivity of the aqueous electrolytic solution phase is varied from 2.6×10^{-4} S cm^{-1} (0.002 M) to 0.25 S cm^{-1} (4.8 M). Each of these solutions was mixed with 100 mg of a silver delafossite powder to form a slurry, which was placed in the measuring apparatus (described elsewhere in detail),[52] and the AC-impedance spectrum was acquired. The application of this technique to materials with known conductivities produces results that are in good agreement with expected values.[52]

Electronic Structure Calculations. Linear muffin-tin orbital (LMTO) calculations[53,54] on the delafossites were performed within the atomic-sphere approximation using version 47C of the *Stuttgart TB-LMTO-ASA* program.[55] Scalar-relativistic Kohn–Sham equations within the local density approximation (LDA)[56] were solved by taking all relativistic effects into account except for the spin–orbit coupling. The calculations were performed on 132 irreducible k points within the primitive wedge of the Brillouin zone. Calculations were performed using an ideal crystal structure of the 2H delafossites (space group $P6_3/mmc$) reported by Kandpal and Seshadri.[57] It has been shown previously that the precise stacking sequence of the delafossites (i.e., 2H or 3R polytype) has little effect on their electronic structure.[58,59]

Results and Discussion

The difficulties normally encountered in the synthesis of silver delafossites were overcome by the Teflon pouch hydrothermal technique.[44] Upon optimization of the reaction temperature and mineralizer concentration, each silver delafossite formed in >90% mass yield in the direct reaction between Ag_2O and the B-site cation sesquioxide or trihydroxide. This method avoids the high temperature and oxygen pressures required previously to synthesize small amounts of both $AgAlO_2$ (crystal)[41] and $AgScO_2$ (powder)[1] delafossites and, indeed, represents a direct method to produce several grams of polycrystalline powder per reaction. Increasing the product yield is necessary for the potential application of silver delafossites as transparent electrodes (laser ablation or sputtering targets) and photocatalysts where large amounts of powder are required. The PXD patterns of the pure-phase silver delafossite samples indexed as either the 3R ($R\bar{3}m$) polytype or a mixture of both the 3R and 2H ($P6_3/mmc$) polytypes (Supporting Information), and the unit cell parameters for each silver delafossite are in agreement with those of previous reports.[1] It should be noted that the orthorhombic β-$AgAlO_2$ and β-$AgGaO_2$ phases,[60] which are
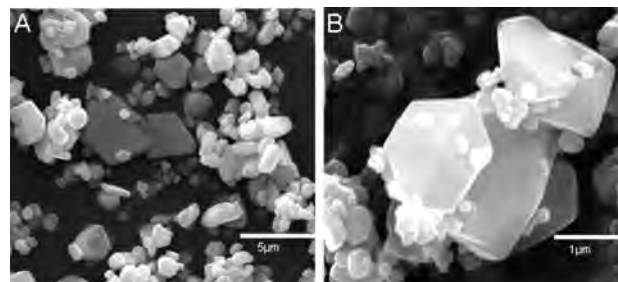
Figure 2. SEM images for (a) a mixture of $AgScO_2$ crystallites ranging in size from a few tenths of one micron up to ~5 μm and (b) a close-up view of some micron-sized hexagonal plates of $AgGaO_2$.
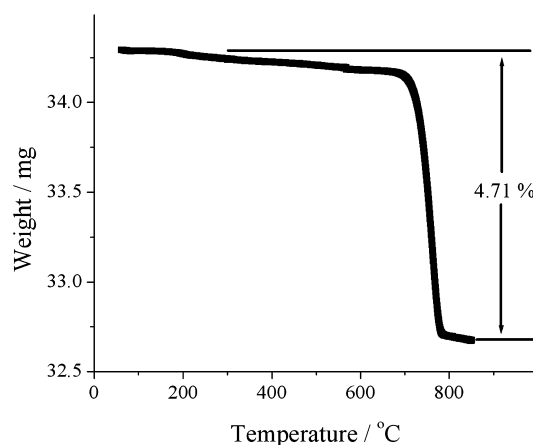
**Figure 3.** Plot of the TGA of $AgAlO_2$ reduced in a N_2 atmosphere. The final products (verified by XRD) were Al_2O_3 and silver metal.

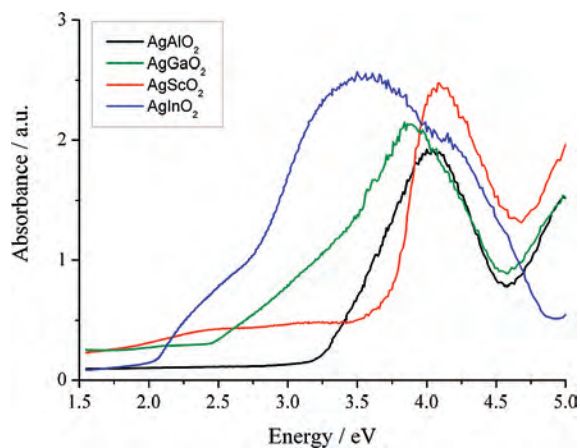common products for cation-exchange reactions involving the smaller B-site cations, were not observed.

The SEM images in Figure 2 illustrate that the particle sizes for silver delafossite crystallites prepared range from 500 nm to a few microns. The cation ratio of each silver delafossite was verified with ICP analysis. For each silver delafossite, the average [Ag]/[B] ratio was 1.02(1). The presence of trace amounts of metallic silver in some product mixtures is not surprising because it has been evidenced in previous attempts at silver delafossite synthesis.[61–66] Prior transmission electron microscopy studies from several commercial vendors reveal Ag_2O to be the source of the silver metal.[43] The oxygen composition of the silver delafossites was verified experimentally by TGA as per eq 1, and the results for $AgAlO_2$ are shown in Figure 3. A 4.71% weight loss is observed beginning at 700 °C. Based on the final products, as characterized by XRD, and the level of weight loss, an initial oxygen content of 2.00(1) per formula unit

(52) Ingram, B. J.; Mason, T. O. *J. Electrochem. Soc.* **2003**, *150*(8), E396–E402.
(53) Andersen, O. K. *Phys. Rev. B: Solid State* **1975**, *12*(8), 3060–3083.
(54) Jepsen, O.; Andersen, O. K. *Z. Phys. B: Condens. Matter* **1995**, *97*(1), 35–47.
(55) Jepsen, O.; Andersen, O. K. *The Stuttgart TB-LMTO-ASA Program*, version 47;MPI fur Festkorperforschung: Stuttgart, Germany, 2000.
(56) Von Barth, U.; Hedin, L. *J. Phys. C: Solid State Phys.* **1972**, *5*(13), 1629–1642.
(57) Kandpal, H. C.; Seshadri, R. *Solid State Sci.* **2002**, *4*(8), 1045–1052.
(58) Seshadri, R.; Felser, C.; Thieme, K.; Tremel, W. *Chem. Mater.* **1998**, *10*(8), 2189–2196.
(59) Ong, K. P.; Bai, K.; Blaha, P.; Wu, P. *Chem. Mater.* **2007**, *19*(3), 634–640.
(60) Gessner, W. *Silikattechnik* **1970**, *21*(2), 45–46.

(61) Wichainchai, A.; Dordor, P.; Doumerc, J. P.; Marquestaut, E.; Pouchard, M.; Hagenmuller, P.; Ammar, A. *J. Solid State Chem.* **1988**, *74*(1), 126–131.
(62) Shin, Y. J.; Doumerc, J. P.; Dordor, P.; Pouchard, M.; Hagenmuller, P. *J. Solid State Chem.* **1993**, *107*(1), 194–200.
(63) Attili, R. N.; Uhrmacher, M.; Lieb, K. P.; Ziegeler, L.; Mekata, M.; Schwarzmann, E. *Phys. Rev. B: Condens. Matter* **1996**, *53*(2), 600–608.
(64) Otabe, T.; Ueda, K.; Kudoh, A.; Hosono, H.; Kawazoe, H. *Appl. Phys. Lett.* **1998**, *72*(9), 1036–1038.
(65) Clayton, J. E.; Cann, D. P.; Ashmore, N. *Thin Solid Films* **2002**, *411*(1), 140–146.
(66) Tate, J.; Jayaraj, M. K.; Draeseke, A. D.; Ulbrich, T.; Sleight, A. W.; Vanaja, K. A.; Nagarajan, R.; Wager, J. F.; Hoffman, R. L. *Thin Solid Films* **2002**, *411*(1), 119–124.
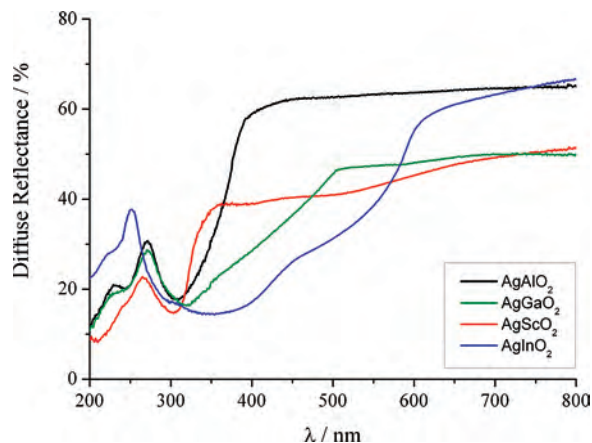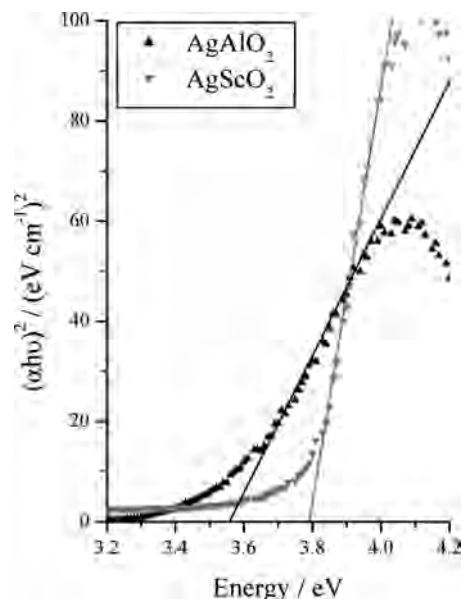
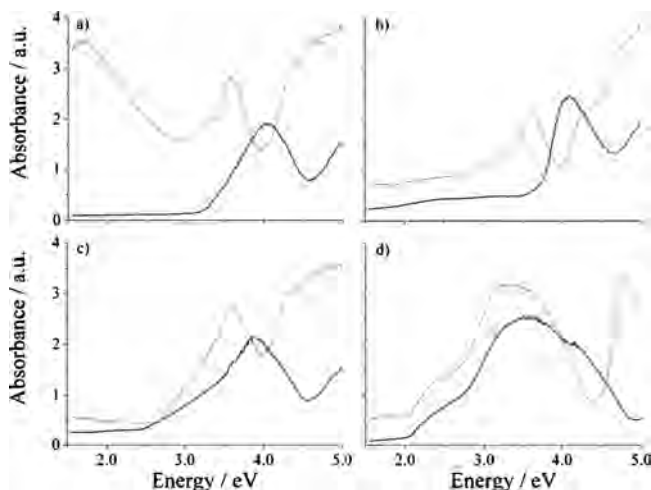**Figure 4.** Diffuse-reflectance spectra of as-prepared silver delafossites.

Figure 5. Kubelka–Munk absorption spectra of as-prepared silver delafossites.

Figure 6. Plot of $(\alpha h\nu)^2$ versus $h\nu$ for AgAlO$_2$ (black) and AgScO$_2$ (gray). The absorption coefficient (α) is estimated by the Kubelka–Munk conversion of diffuse reflectance.


Figure 7. Kubelka–Munk absorption spectra of as-prepared silver delafossites (black lines) compared to their corresponding copper delafossites (gray lines) shown for (a) AAlO$_2$, (b) AScO$_2$, (c) AGaO$_2$, and (d) AInO$_2$.

was measured, consistent with the composition AgAlO$_2$. The calculated oxygen compositions for the other silver delafossites, AgGaO$_2$, AgScO$_2$, and AgInO$_2$, were 2.03, 2.04, and 2.02, respectively (Supporting Information). For the samples of AgGaO$_2$ and AgInO$_2$, a low-temperature weight loss step commencing at 200 °C was observed and can be attributed to the loss of surface water, as determined by IR spectroscopy.[67]

The color of the as-prepared silver delafossites was as follows: white (AgAlO$_2$), light gray (AgScO$_2$), olive green (AgGaO$_2$), and bright orange (AgInO$_2$). To quantify their optical properties, diffuse-reflectance spectra were collected on uniaxially cold-pressed, polycrystalline specimens (150 MPa). The diffuse reflectance (normalized versus a PTFE Halon standard) and converted Kubelka–Munk optical absorbance data are shown in Figures 4 and 5, respectively. Precise determination of the optically measured band gap at Γ, from these plots was complicated because diffuse-reflectance spectroscopy has several inherent limitations when applied to powder samples. First, for crystallite sizes smaller than ~10 μm, Kubelka–Munk theory systematically underestimates the optically measured band gap, with an error

that increases with decreasing crystallite size.[68] Second, while a plot of $(\alpha h\nu)^2$ versus $h\nu$ (Figure 6) can be used to determine the optical band gaps of 3.6 and 3.8 eV for AgAlO$_2$ and AgScO$_2$ samples, respectively, additional light absorption in the visible region for AgGaO$_2$ and AgInO$_2$ samples makes the exact determination of their optical band gaps more challenging. Nonetheless, the optical properties of these silver delafossite are understood by comparing them with data obtained from experimental and computational studies on the copper delafossites, whose optically measured band gaps have been determined accurately from thin film samples.

Figure 7 illustrates that there is a high degree of qualitative similarity between the optical absorption of silver and copper delafossite samples with the same B-site cation. Electronic structure calculations indicate that this similarity results from

(67) Shahriari, D. Y. Ph.D. Thesis, Northwestern University, Evanston, IL, 2004.

(68) Delgass, W. N.; Haller, G. L.; Kellerman, R.; Lunsford, J. H. *Spectroscopy in Heterogeneous Catalysis*; Academic Press Inc. 1979.
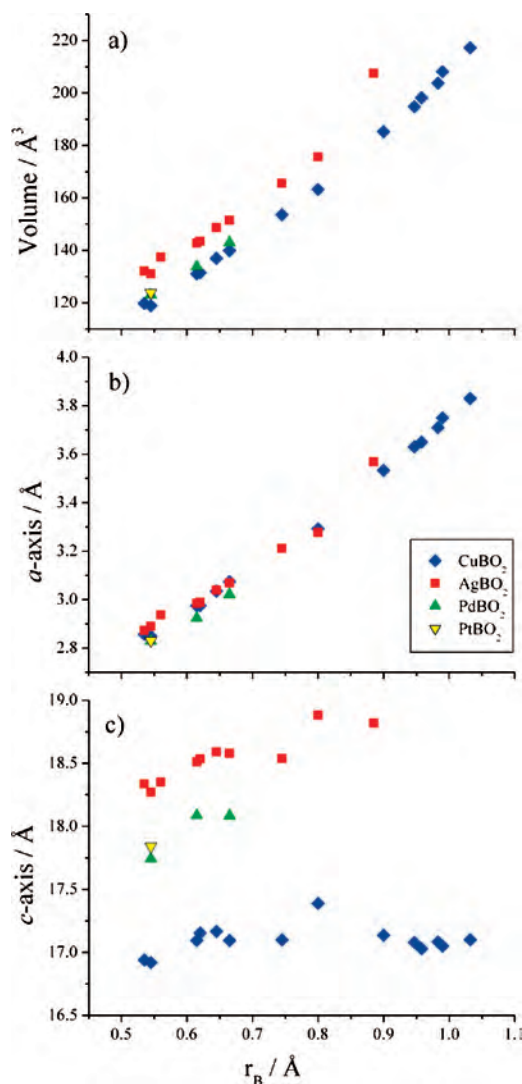
Figure 8. Graph illustrating the relationship between the ionic radius of the B-site cation and (a) the unit cell volume, (b) the *a*-axis length, and (c) the *c*-axis length for delafossites.

a parallel expansion of the unit cell volume for copper and silver delafossites (Figure 8a) when the ionic radius of the group 13 B-site cation increases, 0.535 Å (Al^{3+}) → 0.62 Å (Ga^{3+}) → 0.80 Å (In^{3+}).[38] This parallel unit cell expansion with increasing group 13 B-site cation size decreases the onset energy of a parity-forbidden band-gap transition, resulting in noticeable visible light absorption, and increases the energy of the optically measured band gap. Indeed, the optically measured band gaps for copper delafossites, 3.5 eV ($CuAlO_2$)[69] → 3.6 eV ($CuGaO_2$)[70] → 3.9 eV ($CuInO_2$),[71] and silver delafossites, 3.6 eV ($AgAlO_2$) → 4.1 eV ($AgGaO_2$)[31] → 4.2 eV ($AgInO_2$),[64] expand when the radius of their B-site cation increases. As first noted by Nie et al., however, there is a discrepancy between the above-noted trend in the optically measured band gap of delafossites and most conventional group 13 containing semiconductors, such

as MAs and $CuMS_2$ (M = Al, Ga, and In), whose fundamental direct band gap decreases when the radius of the group 13 element increases.[72] To better understand why the optically measured band gap increases for copper delafossites, Nie et al. applied first-principles methods' LDAs using the full-potential linear augmented plane-wave method to calculate the electronic and optical properties of $CuBO_2$ (B = Al, Ga, and In).[34] On the basis of their calculations, the authors concluded that the fundamental direct band gap at Γ decreases from 2.68 eV ($CuAlO_2$) → 1.64 eV ($CuGaO_2$) → 0.73 eV ($CuInO_2$) and thus does follow the trend observed for conventional group 13 containing semiconductors. Subsequent UV–vis−NIR and X-ray absorption spectroscopic measurements have confirmed that the energies of the forbidden fundamental direct and indirect band gaps decrease down the group.[32,33] As illustrated in Figure 9, our density functional electronic structure calculations using the LMTO method indicate that the fundamental direct band gap of silver delafossites also decreases at Γ from 1.7 eV ($AgAlO_2$) → 1.2 eV ($AgGaO_2$) → 0.6 eV ($AgInO_2$). The decrease in the direct band gap at Γ occurs mainly because the unit cell volume of the delafossites expands with an increase in the size of the B-site cation (Figure 8a), which lowers the energy of the s antibonding states of the group 13 element, thereby decreasing the energy of the conduction band minimum (CBM).[45,73] It should be noted that the LDA-calculated band gaps are consistently underestimated by approximately 0.5–2.0 eV, a level of discrepancy that is not unusual for oxides.[74] The systematic error is expected to cancel, however, because we focus on the difference between band gaps within a group of similar compounds.

The discrepancy between the aforementioned trends in the fundamental direct band gaps and the optically measured band gaps for copper and silver delafossites results from transitions across the fundamental direct band gap being dipole forbidden because both the conduction and valence band states at Γ have the same parity.[34,45] Instead, the optically measured band-gap absorption of a delafossite is determined by the direct band-gap transition at the next lowest energy where the dipolar optical transition matrix element is high. Hence, the optically measured band-gap transition occurs at M for the 2H polytype of delafossite and at L for the 3R polytype, which are assigned to transitions from the valence hybridized copper 3d/silver 4d and oxygen 2p states to copper 4p/silver 5p states (with a lesser contribution from the B-cation ns states) in the conduction band.[45] Unlike the fundamental direct band gap at Γ, the calculated direct band gap at M (Figure 9) widens with an increase in the size of the B-site cation, 3.3 eV ($AgAlO_2$) → 3.2 eV ($AgGaO_2$) → 3.5 eV ($AgInO_2$). The slight decrease at M from $AgAlO_2$ to $AgGaO_2$ is an exception that results from the Ga 4s orbital having much lower energy than that

(69) Yanagi, H.; Inoue, S.-i.; Ueda, K.; Kawazoe, H.; Hosono, H.; Hamada, N. J. *Appl. Phys.* **2000**, *88*(7), 4159–4163.

(70) Ueda, K.; Hase, T.; Yanagi, H.; Kawazoe, H.; Hosono, H.; Ohta, H.; Orita, M. *J. Appl. Phys.* **2001**, *89*(3), 1790–1793.

(71) Yanagi, H.; Hase, T.; Ibuki, S.; Ueda, K.; Hosono, H. *Appl. Phys. Lett.* **2001**, *78*(11), 1583–1585.

(72) Madelung, O.; Schulz, M., *Landolt−Boernstein. Numerical Data and Functional Relationships in Science and Technology*; Springer-Verlag: Berlin, 1987; Vol. 22a.

(73) Robertson, J.; Peacock, P. W.; Towler, M. D.; Needs, R. *Thin Solid Films* **2002**, *411*(1), 96–100.

(74) Eng, H. W.; Barnes, P. W.; Auer, B. M.; Woodward, P. M. *J. Solid State Chem.* **2003**, *175*, 94–109.
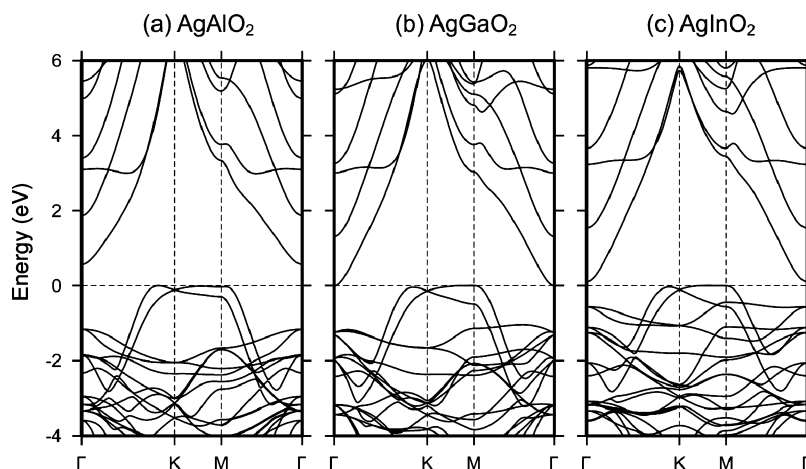
Figure 9. Calculated band structure for (a) AgAlO$_2$, (b) AgGaO$_2$, and (c) AgInO$_2$. Energy zero is at the highest valence band at M.

of the Al 3s orbital.[34] The s orbital contributes to these particular conduction band states and therefore modulates the energy of the CBM. This trend is also observed in the calculated direct band-gap trend at L for 3R polytype copper delafossites, 2.68 eV (CuAlO$_2$) → 2.54 eV (CuGaO$_2$) → 3.08 eV (CuInO$_2$).[34] The energies of these transitions increase with the radius of the B-site cation because the a axis lengthens (Figure 8b) and reduces the A−A interaction in the close-packed A-site cation layer, elevating the conduction band energy of the states with respect to the top of the valence band. Based on the aforementioned band-gap trends of both copper and silver delafossites, it is not surprising that their optically measured band gap expands while their direct band gap decreases when the radius of the B-site cation increases; because their unit cell volumes increase in a similar fashion (Figure 8a).

Despite this increase in the optically measured band gap of delafossites from Al or Ga to In, the previously mentioned low-energy "forbidden" direct band gap at Γ (e.g., 1.2 eV for AgGaO$_2$ and 0.6 eV for AgInO$_2$) results in some measurable absorption of photons in the visible light range, as observed in Figures 4 and 5. Indeed, delafossites, such as CuInO$_2$ and AgInO$_2$ (orange) and CuGaO$_2$ and AgGaO$_2$ (green), are distinctly colored despite having reported band gaps greater than 3.1 eV.[31,64,69,70] Specifically, while the optically measured band gap for a thin film sample of AgGaO$_2$ was reported to be 4.1 eV, there is noticeable light absorption in the transmission spectra of the visible range with a maximum at ∼500 nm (2.5 eV), an energy that corresponds to the onset of light absorption for powder samples of AgGaO$_2$ (Figures 4 and 5).[31] The absorption is significant enough that Maruyama et al. recently reported an optically measured band gap of 2.4 eV for a polycrystalline powder sample of AgGaO$_2$.[24] This reduced band gap and green coloration of AgGaO$_2$ are the result of the "forbidden" direct band-gap transition at Γ and the indirect band gap between Γ and M being partially allowed. Compared to direct and "allowed" band-gap transitions, light absorption owing to a "forbidden" transition increases more
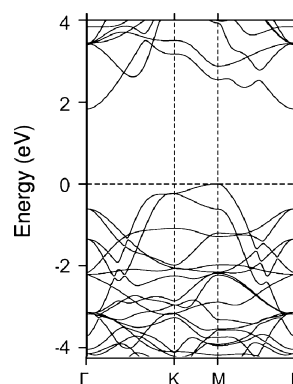
Figure 10. Calculated band structure for AgScO$_2$. Energy zero is at the highest valence band at M.

gradually with energy in the vicinity of the band gap,[75] and significant light absorption can occur when the energy of visible photons is much greater than the energy of a "forbidden" band-gap transition. As expected, the smaller direct band gap at Γ for AgInO$_2$ (0.6 eV) when compared to that for AgGaO$_2$ (1.2 eV), shown in Figure 9, results in the gradual absorption of visible light at a lower energy (2.0 eV) and orange coloration for a powder sample of AgInO$_2$ (Figure 5).

Although the ionic radius of Sc^{3+} (0.745 Å) is between that of Ga^{3+} and In^{3+},[38] the optical properties of AgScO$_2$ are different from those of AgGaO$_2$ and AgInO$_2$. Indeed, the optical absorption data of AgScO$_2$ are more similar to those of AgAlO$_2$, where no significant light absorption is observed in the visible range for powder samples at photon energies less than those for the onset of the optically measured band-gap transition (Figure 5). To better understand the optical properties of AgScO$_2$, LMTO band structure calculations were used to calculate the electronic structure of 2H−AgScO$_2$, which is shown in Figure 10. The fundamental direct band gap at Γ for AgScO$_2$ (2.4 eV) is larger than that of AgGaO$_2$ (1.2 eV) and AgInO$_2$ (0.6 eV) because the CBM of AgScO$_2$ is at higher energy, owing to the lack of 3s electrons for the group 3 B-site cation Sc^{3+}. The 3s orbital contributes to the conduction band states at Γ and

(75) Yu, P. Y., Cardona, M., Eds. *Fundamentals of Semiconductors: Physics and Materials Properties*; Springer, **1995**.
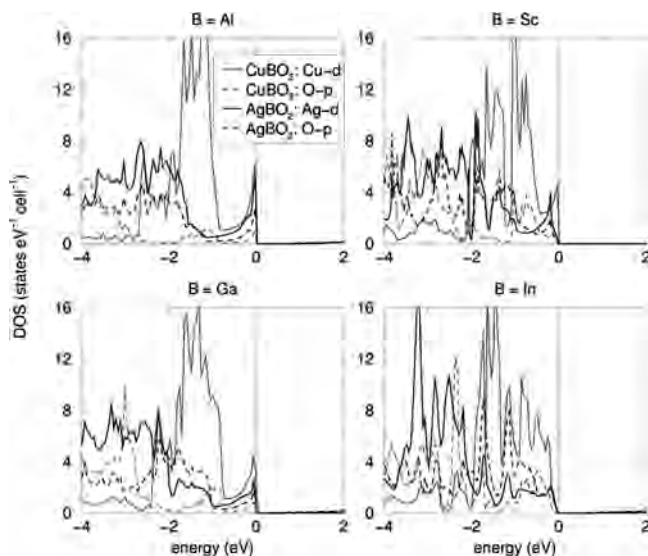
Figure 11. Projected densities of A d and O p states for (a) AAlO$_2$, (b) AScO$_2$, (c) AGaO$_2$, and (d) AInO$_2$, where A = Cu (gray lines) or Ag (black lines). In these plots, the top of the valence band is taken as zero on the energy axis.

therefore modulates the energy of the CBM.[34,45] Therefore, no significant light absorption, resulting from "forbidden" direct or indirect band-gap transitions, occurs in the visible range before the onset of the optically measured band-gap transition of 3.8 eV, which corresponds to the direct band-gap transition at M (Figure 10).

If we now compare copper and silver delafossites with the same B-site cation (Figures 7), one observes that the onset of the optically measured band gaps of the silver delafossites is a few tenths of an electronvolt greater than that of the corresponding copper delafossites. The larger optical band gaps of silver delafossites do not result from the unit cell volume expansion upon replacement of copper with silver on the A site. Because the O–A–O bonds are parallel to the *c* axis, the length of the *a* axis does not change significantly when copper is replaced by silver in a delafossite with a constant B-site cation (Figure 8b). For example, the *a*-axis lengths of CuAlO$_2$ (2.858 Å) and AgAlO$_2$ (2.890 Å) differ by only 0.032 Å, a 1.1% increase. Instead, the unit cell volume increase for silver over copper delafossites with the same B-site cation (Figure 8a) results primarily from an expansion of the *c* axis (Figure 8c). With a minimal change in the *a* axis, the A—A interaction between the closed packed A-site cations should remain constant for copper and silver delafossites with the same B-site cation. If the A—A interaction does not change, the CBM states do not change, leading to the conclusion that the optical gap increases for another reason. Indeed, density functional electronic structure calculations using the LDA LMTO method indicate that the increase of the optical band gap from copper to silver delafossites is due to a change in energy valence band of the optical band gap that includes the A-site cation d states.[57] Figure 11 illustrates that while the partial density of states (PDOS) of copper 3d states is sharply peaked near the top of the valence band, the PDOS for silver 4d states is broader, tails to lower energies, and traces the oxygen p character. The transition of a valence electron from hybridized silver
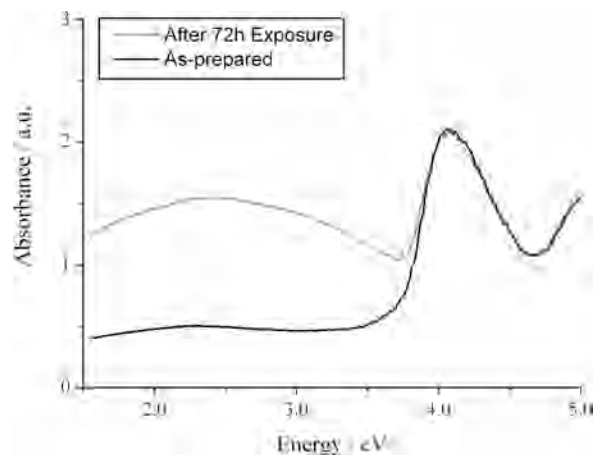
Figure 12. Kubelka–Munk absorption spectra of as-prepared AgScO$_2$ before and after exposure to visible light for 72 h.

4d and oxygen 2p states to silver 5p states in the conduction band thus requires more energy owing to the scarcity of silver 4d states just below the valence band maximum (VBM) of silver delafossites. As a result, silver delafossites have a wider optical band gap compared to the copper delafossites with the same B-site cation (Figure 7). In addition to a larger optical band gap, the as-prepared silver delafossites have lower absorption coefficients than copper delafossites across the visible range. For example, Figure 7a shows that the absorption coefficient of AgAlO$_2$ is one order of magnitude lower than that of CuAlO$_2$. All things considered, the larger band gap and lower absorption coefficients of silver delafossites would translate into more transparent thin films.

The synthesized samples, noticeably AgScO$_2$, exhibit photosensitivity to visible light. This was not surprising because the photochromic behavior of certain silver complex oxides, including AgInO$_2$, has been reported previously.[76] Figure 12 shows the optical absorption data of AgScO$_2$ as-prepared and after continuous exposure to laboratory lighting for 72 h. After light exposure, absorption increases in the visible range at energies less than those of the absorption edge; however, the absorption edge remained constant. The mechanism of the photosensitive properties is analogous to those reported for other complex silver metal oxides where the Ag$^+$ cations reduce to silver metal with the release of oxygen (see eq 1).[76–78] Electron microscopy has revealed previously the presence of globules, which by electron diffraction are shown to be metallic silver, attached to the surface of larger silver oxide particles.[43]

Because the silver delafossite powders could not be sintered into dense ceramics without partial or complete thermal decomposition, a PSC technique[52] was used to measure their electrical properties. The results were analyzed with effective medium theory and equivalent circuit modeling, and the results for AgAlO$_2$ are shown in Figure 13 (see the Supporting Information for PSC data of all silver delafossites). SEM images (Figure 2) showed a similar

(76) Hirono, T.; Yamada, T. *J. Appl. Phys.* **1984**, *55*(3), 781–785.
(77) Gurney, R. W.; Mott, N. F. *Proc. R. Soc. London, Ser. A* **1938**, *164*, 151–167.
(78) L'Vov, B. V. *Thermochim. Acta* **1999**, *333*(1), 13–19.
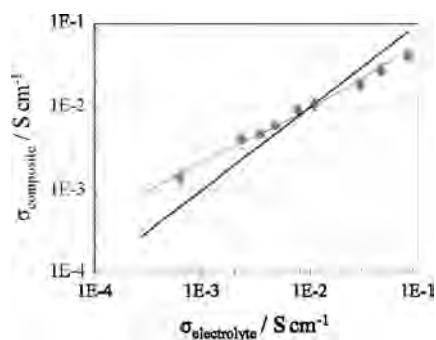
Figure 13. Plot that summarizes the PSC conductivity measurements for $AgAlO_2$. The gray data points represent the measured conductivity of the PSC, while the black line represents the conductivity of the electrolyte solution. A conductivity estimate is given where the composite and electrolyte conductivities are equivalent. A Bruggeman asymmetric model considering randomly arranged spherical particles and a broad range of sizes (volume fraction $\sim$ 0.2–0.3) was used.

Table 1. Measured and Literature Room Temperature Conductivities of Certain Delafossites

compound	form	σ (S cm^{-1})	ref
$CuAlO_2$	crystal	1×10^{-3}	84
$CuAlO_2$	powder	1.7×10^{-3}–3.6×10^{-2}	4, 52, 85
$CuAlO_2$	film	8×10^{-2}–2	30
$AgAlO_2$	powder	9×10^{-3}	this work
$CuGaO_2$	powder	5.6×10^{-3}–1.1×10^{-2}	6, 86
$CuGaO_2$	film	6.3×10^{-2}–0.56	30
$AgGaO_2$	crystal	2×10^{-8}	3
$AgGaO_2$	film	3.2×10^{-4}	31
$AgGaO_2{}^a$	powder	$\leq 10^{-4}$	this work
$CuScO_2$	powder	2×10^{-2}	29
$AgScO_2$	powder	4×10^{-2}	this work
$CuInO_2$	powder	10^{-4}	87
$CuInO_2$	film	5.6×10^{-2}	88
$AgInO_2$	crystal	1×10^{-4}	3
$AgInO_2$	powder	10^{-7}	65
$AgInO_2$	film	1×10^{-5}	64
$AgInO_2$	powder	8×10^{-3}	this work

^{a} The conductivity of the sample is below the measurable range of conductivity ($\leq 10^{-4}$).

platelike morphology for all silver delafossites, and the best fit to the PSC composite data for these particles was given by the model proposed by Fricke in which the Maxwell–Wagner dispersion was extended to a suspension of ellipsoids (platelike).[79] Although some samples were a mixture of two polytypes (2H and 3R), it has been reported previously that the existence of two polytypes, which alters stacking along the c axis, has little effect on the measured polycrystalline conductivity values.[80]

The electrical conductivities of the polycrystalline silver delafossites and other reference delafossites are presented in Table 1. Comparisons of the electrical properties for copper and silver delafossites are complicated by the fact that the carrier type of the silver delafossite powders could not be established reliably. Prior studies of $AgGaO_2$ and $AgInO_2$ have reported thin film samples to be p and n type, respectively, and the small transference number of Ag^+ in such samples, as determined by the direct current polarization method, indicates that ionic contribution to conductivity is negligible.[31,64] While the measured conductivity values are

much lower than typically required for application as a transparent conductor, the conductivities of the as-prepared silver delafossites are comparable to or lower than values previously reported for polycrystalline powder samples of copper delafossites with the same B-site cation (Table 1). Based on the argument of Nagarajan et al. that holes are more mobile in the d states than in the p states,[28] it has been proposed previously that the admixture of oxygen 2p states with the silver 4d states at the VBM (Figure 11) limits the mobility of holes and thus the conductivity of silver delafossites.[57] Indeed, copper delafossites are more conducting because their VBM comprises isolated copper 3d states. Nonetheless, the conductivities of both copper and silver delafossites containing main-group B-site cations are low owing to a diffusion-limited polaron conduction mechanism in which trapped holes and resultant lattice distortions "hop" between sites, which limits room temperature mobility (<1 cm^2 V^{-1} s^{-1}) and therefore conductivity.[45] Similar to copper delafossites, acceptor doping via aliovalent substitution or oxygen intercalation could be used to enhance the conductivity of silver delafossites by increasing the carrier concentration. For example, the conductivities of both $CuYO_2{}^{81,82}$ and $CuCrO_2{}^{83}$ increase significantly upon aliovalent doping with Ca and Mg, respectively.

Conclusions

The silver delafossites $AgAlO_2$, $AgScO_2$, $AgGaO_2$, and $AgInO_2$ have been synthesized on a preparative scale by a low-temperature (<210 °C) and -pressure (<20 atm) Teflon pouch hydrothermal technique. As a result, the optical and electrical properties of a series of these silver delafossites have been examined for the first time. Electronic structure calculations and analysis of the Kubelka–Munk absorption data reveal that, similar to copper delafossites, silver delafossites have a disparity in energy between the "forbidden" fundamental direct and indirect band gaps and optically measured band gap. While their optically measured band gaps widen with an increase in the radius of the B-site cation, the decreased fundamental band gaps for larger B-site cations result in some absorption of photons in the visible light range for $AgGaO_2$ and $AgInO_2$, which reduces their optical transparency and thereby colors these delafossites. When corresponding copper and silver delafossites with the same B-site cation are compared, however, silver delafossites have larger band gaps and lower visible light absorption, owing

(79) Fricke, H. *J. Phys. Chem.* **1953**, *57*, 934–937.

(80) Routbort, J. L.; Rothman, S. J. *J. Appl. Phys.* **1994**, *76*(10), 5615–5628.

(81) Cava, R. J.; Peck, W. F.; Krajewski, J. J.; Cheong, S. W.; Hwang, H. Y. *J. Mater. Res.* **1994**, *9*(2), 314–317.

(82) Jayaraj, M. K.; Draeseke, A.; Tate, J.; Sleight, A. W. *Thin Solid Films* **2001**, *397*, 244–248.

(83) Nagarajan, R.; Draeseke, A. D.; Sleight, A. W.; Tate, J. *J. Appl. Phys.* **2001**, *89*(12), 8022–8025.

(84) Lee, M. S.; Kim, T. Y.; Kim, D. *Appl. Phys. Lett.* **2001**, *79*(13), 2028–2030.

(85) Ingram, B. J.; Gonzalez, G. B.; Mason, T. O.; Shahriari, D. Y.; Barnabe, A.; Ko, D.; Poeppelmeier, K. R. *Chem. Mater.* **2004**, *16*(26), 5616–5622.

(86) Ashmore, N. A.; Cann, D. P. *J. Mater. Sci.* **2005**, *40*, 3891–3896.

(87) Sasaki, M.; Shimode, M. *J. Phys. Chem. Solids* **2003**, *64*(9–10), 1675–1679.

(88) Yang, B.; He, Y.; Polity, A.; Meyer, B. K. *MRS Proc.* **2005**, *865*, 399–403.

to a shift in the valence band states to lower energy upon replacement of copper 3d states with silver 4d states. Thus, we have demonstrated that the electronic structure prediction is general (i.e., any silver delafossite has a larger band gap than the corresponding copper delafossite). Moreover, while silver delafossites have conductivities lower than those of polycrystalline powders of copper delafossites, this study provides a starting point for the difficult process of improving the conductivity of delafossites through extrinsic doping without significantly compromising their optical properties.

Supporting Information Available: Commercial sources and preparation methods for reagents used, PXD spectra matched to calculated PXD patterns generated from published crystallographic data, TGA data, and PSC conductivity data and references. This material is available free of charge via the Internet at http://pubs.acs.org.

IC702197H